Medical Physics
The International Journal of Medical Physics Research and Practice

# Characterization of a water-equivalent fiber-optic coupled dosimeter for use in diagnostic radiology

Daniel E. Hyer, Ryan F. Fisher, and David E. Hintenlang

Citation: Medical Physics **36**, 1711 (2009); doi: 10.1118/1.3116362
View online: http://dx.doi.org/10.1118/1.3116362
View Table of Contents: http://scitation.aip.org/content/aapm/journal/medphys/36/5?ver=pdfcov
Published by the American Association of Physicists in Medicine



# Characterization of a water-equivalent fiber-optic coupled dosimeter for use in diagnostic radiology

Daniel E. Hyer,[a] Ryan F. Fisher, and David E. Hintenlang
*University of Florida, 202 Nuclear Sciences Center, P.O. Box 118300, Gainesville, Florida 32611*

(Received 7 January 2009; revised 25 February 2009; accepted for publication 18 March 2009; published 16 April 2009)

This work reports on the characterization of a new fiber-optic coupled (FOC) dosimeter for use in the diagnostic radiology energy range. The FOC dosimeter was constructed by coupling a small cylindrical plastic scintillator, 500 $\mu$m in diameter and 2 mm in length, to a 2 m long optical fiber, which acts as a light guide to transmit scintillation photons from the sensitive element to a photomultiplier tube (PMT). A serial port interface on the PMT permits real-time monitoring of light output from the dosimeter via a custom computer program. The FOC dosimeter offered excellent sensitivity and reproducibility, allowing doses as low as 0.16 mGy to be measured with a coefficient of variation of only 3.64%. Dose linearity was also excellent with a correlation coefficient of 1.000 over exposures ranging from 0.16 to 57.29 mGy. The FOC dosimeter exhibited little angular dependence from axial irradiation, varying by less than 5% over an entire revolution. A positive energy dependence was observed and measurements performed within a scatter medium yielded a 10% variation in sensitivity as beam quality changed due to hardening and scatter across a 16 cm depth range. The current dosimetry system features an array of five PMTs to allow multiple FOC dosimeters to be monitored simultaneously. Overall, the system allows for rapid and accurate dose measurements relevant to a range of diagnostic imaging applications. © *2009 American Association of Physicists in Medicine*. [DOI: 10.1118/1.3116362]

Key words: point radiation detector, organ dose, dosimetry, diagnostic radiology

## I. INTRODUCTION

Interest in accurately quantifying the absorbed dose from diagnostic procedures by performing in-phantom or *in vivo* dose measurements has prompted the development of a new fiber-optic coupled (FOC) dosimeter. The FOC architecture was chosen due to its small size and ability to provide real-time dose information during irradiation. Other dosimeters commonly used in diagnostic radiology, such as ionization chambers, thermoluminescent dosimeters (TLDs), or optically stimulated luminescent (OSL) dosimeters are either too large to incorporate into phantoms or require a time consuming reading process after irradiation to extract dose information. Additionally, TLDs have shown an angular dependence of up to 20%,[1] while OSLs have shown degradation with repeated exposures.[2] Metal-oxide field-effect transistors (MOSFETs) have also been investigated for use in diagnostic radiology, but reproducibility variations as high as 15%–30% (Ref. 3) between measurements, along with metallic components which can lead to image artifacts, have limited their success. Lastly, diode detectors have been investigated but are too large for in-phantom measurements and suffer from an over-response to low energy photons and an angular dependence of as great as 50%.[4] The over-response to low energy photons is of particular concern because low energy scatter inside a phantom could lead to inaccurate dose measurements when utilizing such a system for in-phantom dosimetry. It is important to note, however, that this characteristic is not unique to diode detectors. Any detector composed of high-$Z$ materials, including TLDs, OSLs, and MOSFETs, will over-respond to low energy photons in the diagnostic spectra due to the strong atomic number dependence of radiation interactions (mainly photoelectric) at these energies.

FOC dosimeters, utilizing a variety of sensitive elements, have seen some success in both diagnostic and therapeutic applications. They overcome many of the shortfalls of other dosimeter systems by showing little angular dependence, no detectable performance degradation over time, high reproducibility, and real-time output while maintaining a small physical size that allows measurements with high spatial resolution. In diagnostic and mammographic applications, FOC dosimeters utilizing a copper-doped quartz sensitive element have been utilized, but calibration and reproducibility concerns remain.[5,6] In therapeutic applications, FOC dosimeters utilizing a water-equivalent plastic scintillator as the sensitive element have been used, along with gating or filters to eliminate the effects of Cerenkov radiation, for dose verification in several applications.[7,8]

This study extends the use of water-equivalent plastic scintillator based FOC dosimeters to diagnostic applications, where energies are low enough (less than 190 keV for silica) that the production of Cerenkov radiation in the optical fiber is not a concern.[9] Plastic scintillation material was chosen as the sensitive element of the FOC dosimeter in this study for two primary reasons: An adequate light output to maintain a high signal-to-noise ratio and a water-equivalent effective $Z$. The water-equivalent effective $Z$ prevents image artifacts and mimics the radiation interaction properties of soft tissue,

 0094-2405/2009/36(5)/1711/6/$25.00  


FIG. 1. Completed FOC dosimeter.

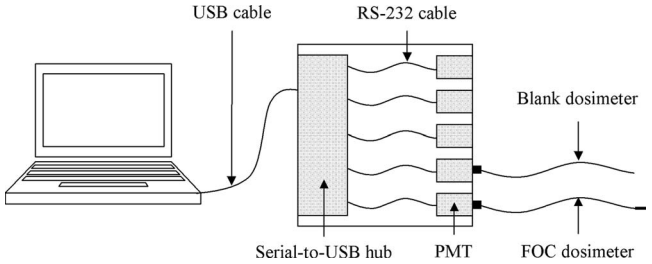


FIG. 2. FOC dosimetry system schematic, power supplies for serial-to-USB hub, and PMTs not shown.

eliminating the over-response to low energy photons and producing an energy dependence that allows for easy and effective calibration.

The FOC dosimeter was constructed by coupling a small cylindrical plastic scintillator, 500 $\mu$m in diameter and 2 mm in length, to a 2 m long optical fiber, which acts as a light guide to transmit scintillation photons from the sensitive element to a photomultiplier tube (PMT). A serial port interface on the PMT permits real-time monitoring of dosimeter output via a custom computer program. To allow multiple FOC dosimeters to be monitored simultaneously, an array of five PMTs was constructed. The end result of this work is a multichannel fiber-optic coupled dosimetry system capable of accurately measuring in-phantom doses in the diagnostic energy range with real-time resolution.

## II. MATERIALS AND METHODS

### II.A. FOC dosimetry system

The sensitive element of the FOC dosimeter consists of a water-equivalent plastic scintillator (BCF-12, Saint-Gobain Crystals, Nemours, France) in the shape of a cylinder with a diameter of 500 $\mu$m and a length of 2 mm. To transmit the scintillation photons from the sensitive element to a PMT, the scintillator was mechanically coupled to an unjacketed optical fiber (400-UV, Ocean Optics Inc., Dunedin, FL) with a diameter of 400 $\mu$m and a length of 2 m using a short piece ($\sim$1 cm) of heat shrink tubing. To maximize the number of scintillation photons reaching the PMT, the coupled ends of both the scintillator and optical fiber were polished, as suggested by Ayotte *et al.*,[10] with progressively finer lapping films (12, 3, and 1 $\mu$m). The uncoupled end of the scintillator was similarly polished and then coated with a reflective paint (EJ-510, Eljen Technology, Sweetwater, TX) in order to prevent the escape of scintillation photons, effectively increasing the output of the sensitive element.[11] At the opposite end of the optical fiber, a female SMA 905 connecter (SMA-490, Ocean Optics Inc., Dunedin, FL) was installed to enable the FOC dosimeter to be connected with a PMT. Lastly, the entire FOC dosimeter was wrapped in opaque heat shrink tubing to restrict ambient light and add strength to the assembly. A completed FOC dosimeter is shown in Fig. 1.

While the majority of the light reaching the PMT is a result of photons released from the sensitive element of the FOC dosimeter, a fraction of the light is a result of the native fluorescence within the optical fiber itself.[7,12] The fluorescence of the optical fiber is commonly referred to as the stem effect, and if not accounted for can result in significant errors in dose measurements. In order to account for this effect, a second blank dosimeter was constructed without a sensitive element. For the purposes of this study, the blank dosimeter was placed next to the FOC dosimeter during all exposure measurements and the stem effect was measured and subtracted from the FOC dosimeter output. As used in this study, the blank dosimeter typically accounted for less than 10% of the total counts measured via the FOC dosimeter.

To facilitate the simultaneous reading of multiple FOC or blank dosimeters, an array of five photon counting PMTs (H7467, Hamamatsu Corporation, Bridgewater, NJ) was fabricated. While only one FOC dosimeter was used for this study, the capability of reading multiple dosimeters simultaneously will greatly increase the speed of data collection for future work such as anthropomorphic phantom organ dose measurements. To limit the number of spurious pulses detected due to scattered x rays reaching the PMTs and causing photocathode emissions, the box housing the PMT array was lined with 1/16 in. lead shielding. A male SMA optical fiber adapter (E5776–51, Hamamatsu Corporation, Bridgewater, NJ) was also fitted to each PMT to enable connection with an FOC dosimeter. Counting data from each PMT was routed through a serial-to-USB hub (UPort 1610–8, Moxa Inc., Brea, CA) via RS-232 cables and subsequently transferred from the hub to a laptop computer via a USB cable. A custom MATLAB® (Mathworks Inc., Natick, MA) computer program was developed to interface with the PMT array and provide real-time monitoring of dosimeter output. For clarification, a simplified schematic of the entire FOC dosimetry system is shown in Fig. 2. Components not shown include a 5 V DC power supply for the PMT modules and a 12 V DC power supply for the serial-to-USB hub.

### II.B. Exposure measurements

Unless otherwise noted, the characterization of the FOC dosimeter was performed using a clinical x-ray tube with a measured half value layer of 5.76 mm of Al at 120 kVp and a fixed field size of $20\times20$ cm$^2$. All testing, except for the angular dependence which was done free-in-air, was performed with the dosimeter placed on top of a polymethyl methacrylate (PMMA) slab to provide a backscatter medium. All measurements were repeated five times to reduce statis-

tical uncertainties and provide reproducibility metrics. A 15 $cm^3$ pancake ion chamber and associated electrometer (chamber model 96035B, electrometer model 35050A, Keithley Instruments Inc., Cleveland, OH) were used to provide simultaneous exposure measurements.

It should be noted that all results reported in this study have been corrected for the stem effect with the use of a blank dosimeter. A calibration between the PMT used for the FOC dosimeter and the PMT used for the blank dosimeter was also performed to eliminate the influence of sensitivity differences between the two PMTs.

### II.C. Energy dependence

The energy dependence of the FOC dosimeter was evaluated by incrementally increasing the tube potential from 40 to 120 kVp in 10 kVp increments while maintaining the current-time product constant at 50 mA s. The ion chamber was placed next to the FOC dosimeter and irradiated simultaneously to provide a reading of the air kerma from each exposure. These data were then used to plot the normalized dosimeter sensitivity, in counts/mGy, versus tube potential.

To evaluate the effect of varying beam quality as a function of tissue depth due to beam hardening and scattering, varying thicknesses of soft tissue-equivalent material[13] were placed on top of both the FOC dosimeter and ion chamber and exposures were taken at 120 kVp and 50 mA s with a fixed field size of $10\times10$ $cm^2$. These data were then used to create a plot of the normalized dosimeter sensitivity, in counts/mGy, versus depth in the soft tissue-equivalent material.

### II.D. Linearity

The linearity of the FOC dosimeter was evaluated by increasing the current-time product from 0.5 to 160 mA s while keeping the tube potential constant at 120 kVp, yielding air kerma values ranging from 0.16 to 57.29 mGy. The current-time product was initially varied by holding the exposure time constant and adjusting the tube current. Unfortunately, the entire dose range desired could not be achieved with a single exposure time setting, and therefore several different exposure times were utilized (20, 50, 100, 200, and 320 ms). By holding the exposure time constant when possible, the dose rate was effectively varied and therefore the results also indicate the dose rate linearity of the FOC dosimeter. A linear fit was applied to a plot of the FOC dosimeter's counts versus measured air kerma and the correlation coefficient was used to quantify the linearity of the dosimeter.

### II.E. Reproducibility

The reproducibility of the FOC dosimeter was evaluated using the data from the linearity experiment. Because each measurement was repeated five times, the data provided an adequate sample from which to take average readings and standard deviation for different exposure levels of interest in diagnostic radiology. The coefficient of variation (COV) at each exposure level was calculated to quantify the dosimeter's reproducibility.

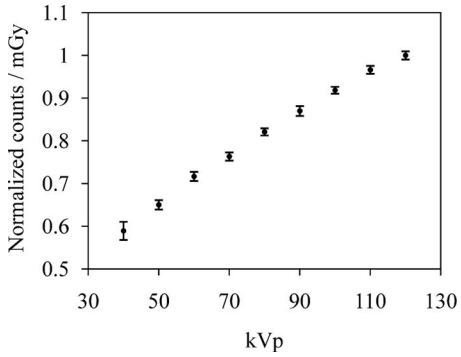


FIG. 3. Energy dependence of FOC dosimeter. Data have been normalized to the data point at 120 kVp. Error bars correspond to ±1 standard deviation of the mean.

### II.F. Dosimeter response versus bend radius

The change in response of the FOC dosimeter as the optical fiber was bent to various radii was also investigated. Technique settings were fixed at 120 kVp and 50 mA s. The dosimeter was first irradiated with the optical fiber straight to obtain a baseline value. The dosimeter was then irradiated with the optical fiber bent into a single loop 20 cm in radius at a distance of 40 cm from the sensitive element of the dosimeter. Measurements were repeated with progressively smaller loop radii (10, 7.5, 4, and 2.5 cm) to fully characterize the response of the dosimeter versus bend radius of the optical fiber.

### II.G. Angular dependence

The angular dependence of the FOC dosimeter was evaluated using a clinical computed tomography (CT) unit with a half value layer of 7.0 mm of Al at 120 kVp. Static shots at fixed tube angles were taken with technique settings of 120 kVp and 5 mA s. A CT unit was chosen for this testing because it provided an easy method of accurately obtaining the response of the dosimeter as a function of angle of incident radiation. The dosimeter was first placed at the isocenter of the unit free-in-air with the patient table out of the beam and irradiated axially (around the cylindrical axis of the dosimeter). Measurements were made at intervals of 30° all the way around the dosimeter. The dosimeter was then turned and irradiated normal-to-axial, where 0° corresponds to x rays incident on the tip of the dosimeter and 180° corresponds to x rays incident from the back side of the dosimeter. Again, measurements were made at intervals of 30°.

## III. RESULTS

### III.A. Energy dependence

Figure 3 plots the normalized sensitivity of the FOC dosimeter, in counts/mGy, as a function of tube potential. The results were normalized to the measurement point at 120

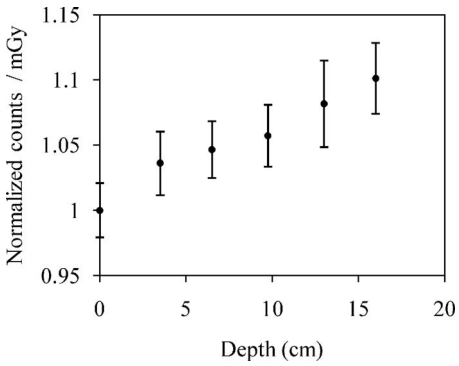


FIG. 4. Energy dependence of FOC dosimeter as a function of depth in soft tissue-equivalent material. Data have been normalized to the surface measurement (depth=0), which corresponds to the 120 kVp measurement in Fig. 3. Error bars correspond to ±1 standard deviation of the mean.

kVp for ease in comparison. As can be seen, the energy response is fairly linear and the sensitivity of the FOC dosimeter increases an average of 6.8%/10 kVp across the energy range shown.

Additionally, Fig. 4 plots the normalized sensitivity of the FOC dosimeter, in counts/mGy, as a function of depth in soft tissue-equivalent material. The results were normalized to the surface measurement point, which corresponds to the 120 kVp measurement point in Fig. 3, for ease in comparison. As the depth increases, the x-ray spectrum changes due to beam hardening and the addition of a scatter component. This effect causes the sensitivity of the dosimeter to vary due to its energy dependence. However, the variation is only 10% across the depth range investigated.

### III.B. Linearity

Figure 5 plots the response of the FOC dosimeter, in counts, as a function of air kerma, in mGy. Error bars are not shown because they were too small to be displayed. A linear trend line was fitted to the data and the correlation coefficient was found to be 1.000. This result demonstrates that the FOC dosimeter has a very linear response over the exposure range of interest in diagnostic radiology.

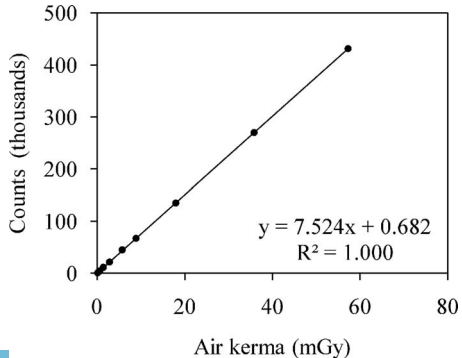


FIG. 5. Dose linearity of FOC dosimeter.

TABLE I. Reproducibility of measurements with FOC dosimeter.

| Air kerma (mGy) | Mean counts (net) | Standard deviation | COV (%) |
|---|---|---|---|
| 0.16 | 1315 | 48 | 3.64 |
| 0.30 | 2523 | 58 | 2.30 |
| 0.60 | 4895 | 50 | 1.03 |
| 1.46 | 11 891 | 107 | 0.90 |
| 2.85 | 22 076 | 280 | 1.27 |
| 5.76 | 45 405 | 290 | 0.64 |
| 8.91 | 67 768 | 491 | 0.72 |
| 17.96 | 135 556 | 247 | 0.18 |
| 35.81 | 270 178 | 1046 | 0.39 |
| 57.29 | 431 655 | 2862 | 0.66 |

### III.C. Reproducibility

Table I summarizes the average readings and standard deviation, in counts, over the exposure range of interest commonly used in diagnostic radiology. The coefficient of variation was less than 1% for most exposure levels, demonstrating that the FOC dosimeter is capable of highly reproducible readings. As expected, the variation was slightly higher at low exposure levels due to less total counts and more fluctuations between readings. However, the coefficient of variation was only 3.64% for even the lowest exposure level (0.16 mGy).

### III.D. Dosimeter response versus bend radius

Figure 6 plots the response of the FOC dosimeter as the optical fiber was bent into a single circular loop with progressively smaller radii. The response was normalized to the measurement point in which the optical fiber was straight for ease of comparison. The response of the dosimeter remained relatively constant for large bend radii and did not decrease significantly (>10%) until a small radius of 2.5 cm was obtained.

### III.E. Angular dependence

Figures 7 and 8 plot the response of the FOC dosimeter to an axial and normal-to-axial irradiation free-in-air, respec-

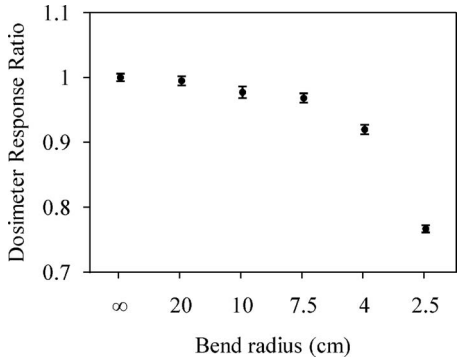


FIG. 6. Response of FOC dosimeter versus the bend radius of the optical fiber. Data have been normalized to a bend radius of infinity. Error bars correspond to ±1 standard deviation of the mean.

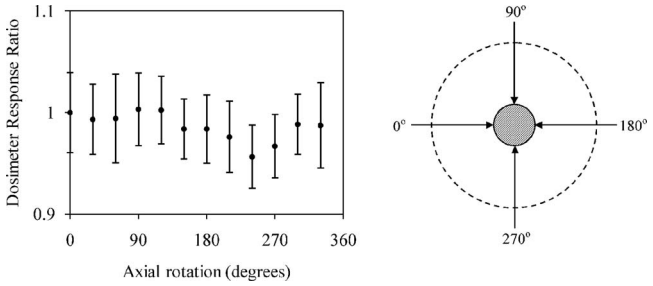


FIG. 7. Angular dependence of FOC dosimeter to an axial irradiation. Data have been normalized to a zero-degree axial angular response. Error bars correspond to ±1 standard deviation of the mean. Experimental setup is also shown. Shaded area represents a head on view of the sensitive element of the FOC dosimeter.

tively. All data were normalized to a 0° axial irradiation for ease of comparison. For the normal-to-axial data, 0° corresponds to x rays incident on the distal tip of the dosimeter and 180° corresponds to x rays incident from the backside of the dosimeter. As expected due to the cylindrical geometry, the response of the dosimeter showed little angular dependence to an axial irradiation, varying by less than 5% over an entire revolution. The response of the dosimeter to a normal-to-axial irradiation showed a reduction of 97% in the number of counts detected when the x rays were incident through a narrow range of angles directly from the back of the dosimeter (180°). A slight reduction in recorded counts of approximately 12% was also seen when radiation was incident on the face of the dosimeter (0°).

## IV. DISCUSSION

The FOC dosimeter showed excellent dose linearity and reproducibility when benchmarked against an ion chamber. Additionally, there was minimal reduction in dosimeter's response as the optical coupling fiber was bent into loops of decreasing radius. At a bend radius of 2.5 cm a significant reduction was seen, but such a tight bend radius is far beyond the range expected to be encountered with the normal use of the FOC dosimetry system.

The FOC dosimeter exhibited positive energy dependence in the range of tube potentials evaluated (40–120 kVp). Initially, it was thought that energy or beam quality dependent calibration factors could be used to simply correct for this effect. However, it was later realized that when using the dosimeter for in-phantom dosimetry, depth-dependent correction factors may also be needed to account for the energy dependence of the dosimeter due to variations in beam quality at increasing depths as a result of beam hardening and the addition of a scatter component. The need for depth-dependent correction factors was evaluated, as shown in Fig. 4, and it was found that the sensitivity of the dosimeter varied by only 10% over the depth range investigated. Much of this variation occurred between the free-in-air measurement (depth=0) and the first data point in tissue, suggesting that the dosimeter could be calibrated under only a few cm of scattering medium to minimize the effect of the dosimeters energy dependence for in-phantom dose measurements. It should be noted that specific irradiation geometries and conditions should be evaluated similarly in order to determine the extent to which changes in the beam energy spectrum could affect the dosimeter's calibration. Also, this issue is not unique to only the FOC dosimetry system, but applies to many dosimeters commonly used in diagnostic measurements (TLDs, OSLs, MOSFETs, and diodes, for example), though the issue is seldom investigated or accounted for in the current literature.

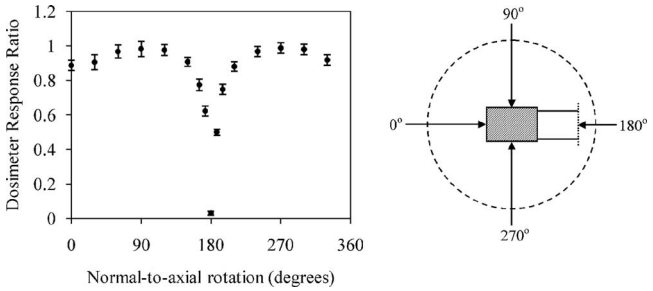


FIG. 8. Angular dependence of FOC dosimeter to a normal-to-axial irradiation. Data have been normalized to a zero-degree axial angular response. Error bars correspond to ±1 standard deviation of the mean. Experimental setup is also shown. Shaded area represents a side view of the sensitive element of the FOC dosimeter.

The angular dependence of the FOC dosimeter was evaluated for both axial and normal-to-axial irradiations. Due to the cylindrical geometry of the dosimeter, little angular dependence was expected from an axial irradiation. Figure 7 demonstrates this result, showing that the dosimeter's response varied by less than 5% over an entire revolution. This small amount of variation can be attributed to the construction of the dosimeter, as it is technically difficult to ensure that the sensitive element is perfectly aligned with the optical fiber. Because angular dependence is a function of the alignment of the sensitive element, each dosimeter should be characterized prior to its initial clinical use. The response of the dosimeter to a normal-to-axial irradiation showed a reduction in counts of 97% when irradiated from the back side due to attenuation of x rays by the optical fiber itself. Additionally, the response of the dosimeter dropped by 12% when radiation was incident on the distal tip of the dosimeter. This reduction is attributable to the smaller solid angle provided by the cylindrical geometry of the sensitive element when viewed head on. The variations in detector's response can be minimized in projection radiography with proper orientation of the dosimeter. In CT dosimetry, the effects of these variations will likely be averaged out for in-phantom measurements due to the rotation of the x-ray tube. In order to illustrate this point, the area under the curve shown in Fig. 8 was found to be only 11% less than that of an ideal detector response with no angular dependence. In addition, the presence of scatter radiation has been found to reduce the effects of angular dependence in in-phantom dose measurements.[14]

## V. CONCLUSIONS

The FOC dosimeter described in this study offers immediate readout, excellent sensitivity, linear dose response, and high reproducibility in a physical package that is small enough to be used for in-phantom or *in vivo* dose measurements. Additionally, the FOC dosimeter showed no significant decrease in response as the optical fiber was bent for radii commonly seen during clinical use. Drawbacks of this dosimeter include positive energy dependence and a decrease in response for irradiations incident from the back of the dosimeter. However, the energy dependence is minimized by calibrating the dosimeter under several cm of material to account for changing beam quality with depth due to beam hardening and scattering. Variations in angular response can be minimized by proper orientation of the dosimeter in projection radiography and will be negligible for in-phantom measurements in CT imaging as variations will be reduced by the presence of scatter radiation and the rotation of the x-ray tube. Overall, the FOC dosimetry system provides rapid and accurate dose measurements applicable to a range of diagnostic imaging applications, with particular utility for in-phantom CT organ dose measurements.

## ACKNOWLEDGMENT

This work was supported by the U.S. Department of Energy under project Award No. DE-GF07-05ID14700.

[a]Electronic mail: hyer717@ufl.edu

[1]L. Struelens, F. Vanhavere, and K. Smans, "Experimental validation of Monte Carlo calculations with a voxelized Rando-Alderson phantom: A study on influence parameters," Phys. Med. Biol. **53**, 5831–5844 (2008).

[2]J. M. Edmund and C. E. Anderson, "Temperature dependence of the $Al_2O_3$:C response in medical luminescence dosimetry," Radiat. Meas. **42**, 177–189 (2007).

[3]L. A. Benevides and D. E. Hintenlang, "Characterization of metal oxide semiconductor field effect transistor dosimeters for application in clinical mamography," Med. Phys. **33**, 514–520 (2006).

[4]T. Aoyama, S. Koyama, and C. Kawaura, "An in-phantom dosimetry system using pin silicon photodiode radiation sensors for measuring organ doses in x-ray CT and other diagnostic radiology," Med. Phys. **29**, 1504–1510 (2002).

[5]L. A. Benevides, A. L. Huston, B. L. Justus, P. Falkenstein, L. F. Brateman, and D. E. Hintenlang, "Characterization of a fiber-optic-coupled radioluminescent detector for application in the mammography energy range," Med. Phys. **34**, 2220–2227 (2007).

[6]A. K. Jones and D. E. Hintenlang, "Potential clinical utility of a fibre optic-coupled dosemeter for dose measurements in diagnostic radiology," Radiat. Prot. Dosim. **132**, 80–87 (2008).

[7]B. L. Justus, P. Falkenstein, A. L. Huston, M. C. Plazas, H. Ning, and R. W. Miller, "Gated fiber-optic-coupled detector for in vivo real-time radiation dosimetry," Appl. Opt. **43**, 1663–1668 (2004).

[8]F. Lacroix, L. Archambault, L. Gingras, M. Guillot, A. S. Beddar, and L. Beaulieu, "Clinical prototype of a plastic water-equivalent scintillating fiber dosimeter array for QA applications," Med. Phys. **35**, 3682–3690 (2008).

[9]M. R. Arnfield, "Radiation-induced light in optical fibers and plastic scintillators: Application to brachytherapy dosimetry," IEEE Trans. Nucl. Sci. **43**, 2077–2084 (1996).

[10]G. Ayotte, L. Archambault, L. Gingras, F. Lacroix, A. S. Beddar, and L. Beaulieu, "Surface preparation and coupling in plastic scintillator dosimetry," Med. Phys. **33**, 3519–3525 (2006).

[11]J. Elsey, D. R. McKenzie, J. Lambert, N. Suchowerska, S. L. Law, and S. C. Fleming, "Optimal coupling of light from a cylindrical scintillator into an optical fiber," Appl. Opt. **46**, 397–404 (2007).

[12]C. J. Marckmann, M. C. Aznar, C. E. Andersen, and L. Botter-Jensen, "Influence of the stem effect on radioluminescence signals from optical fibre $Al_2O_3$:C dosemeters," Radiat. Prot. Dosim. **119**, 363–367 (2006).

[13]R. F. Fisher, MS thesis, University of Florida, 2006.

[14]W. E. Moloney, MS thesis, University of Florida, 2008.